Calcium-Induced Conformational Changes in the C-Terminal Half of Gelsolin Stabilize Its Interaction with the Actin Monomer†

Sofia Khaitlina,‡ Markus Walloscheck,§ and Horst Hinssen*,§

Biochemical Cell Biology Group, University of Bielefeld, D 33501 Bielefeld, Germany, and Institute of Cytology, Russian Academy of Sciences, 196064 St. Petersburg, Russia

Received March 7, 2004; Revised Manuscript Received June 6, 2004

ABSTRACT: The basic mechanism for the nucleating effect of gelsolin on actin polymerization is the formation of a complex of gelsolin with two actin monomers. Probably due to changes in the C-terminal part of gelsolin, a stable ternary complex is only formed at $[Ca^{2+}] > 10^{-5}$ M [Khaitlina, S., and Hinssen, H. (2002) *FEBS Lett. 521*, 14−18]. Therefore, we have studied the binding of actin monomer to the isolated C-terminal half of gelsolin (segments 4−6) over a wide range of calcium ion concentrations to correlate the conformational changes to the complex formation. With increasing $[Ca^{2+}]$, the apparent size of the C-terminal half as determined by gel filtration was reduced, indicating a transition into a more compact conformation. Moreover, Ca^{2+} inhibited the cleavage by trypsin at Lys 634 within the loop connecting segments 5 and 6. Though the inhibitory effect was observed already at $[Ca^{2+}]$ of 10^{-7} M, it was enhanced with increasing $[Ca^{2+}]$, attaining saturation only at $>10^{-4}$ M Ca^{2+}. This indicates that the initial conformational changes are followed by additional molecular transitions in the range of 10^{-5}−10^{-4} M $[Ca^{2+}]$. Consistently, preformed complexes of actin with the C-terminal part of gelsolin became unstable upon lowering the calcium ion concentrations. These data provide experimental support for the role of the type 2 Ca-binding sites in gelsolin segment 5 proposed by structural studies [Choe et al. (2002) *J. Mol. Biol. 324*, 691]. We assume that the observed structural transitions contribute to the stable binding of the second actin monomer in the ternary gelsolin−actin complex.

Gelsolin is an actin-binding protein that nucleates actin polymerization and severs and caps actin filaments. All of these properties are strongly Ca-dependent (for a recent review, see ref *1*). At $[Ca^{2+}] < 10^{-7}$ M, no gelsolin−actin interaction has been observed. At 10^{-7}−10^{-6} M Ca^{2+}, gelsolin undergoes conformational changes that are sufficient for at least one actin monomer to be bound (*2*−*5*). However, a stable complex of gelsolin with two actin monomers is formed only at $[Ca^{2+}] > 10^{-5}$ M (*5*). This is in good agreement with the Ca^{2+} concentrations required for severing of actin filaments and nucleation of actin polymerization (*6*−*8*).

Gelsolin consists of six homologous domains (segments 1−6). In the ternary complex one actin monomer is bound in each half of the molecule (segments 1−3 for the N-terminal half and segments 4−6 for the C-terminal half). The two actin monomers bound are not functionally equivalent. Although the structure of the N-terminal part of gelsolin is modified by Ca^{2+} (*5*, *9*, *10*), interaction of the actin monomer with the N-terminal half is largely Ca-insensitive, whereas its binding to the C-terminal part was shown to occur only in the presence of Ca^{2+} (*11*). In addition, the monomer interacting with the C-terminal part of gelsolin is exchangeable (*11*). This implies that stable binding of the second actin monomer in the ternary actin/gelsolin complex can be associated with Ca-induced conformational changes in the C-terminal half of gelsolin. The Ca-induced structural transitions of the C-terminal half of gelsolin were evident both from measurements of dynamic light scattering (*12*) and from analysis of its crystal structure (*13*, *14*). Analysis of the structure of Ca-activated gelsolin in both the presence and absence of actin clearly showed that the major conformational changes are all induced by Ca binding and not by binding of actin (*14*−*16*). However, none of the sites involved in this transition have been localized. Moreover, the effects were registered at high calcium concentrations (100 μM), and no data about conformational changes of the gelsolin C-terminal half and actin binding at lower $[Ca^{2+}]$ are available. Therefore, the aim of this work was to elucidate the interaction of the C-terminal half of gelsolin with actin monomer in a wide range of Ca^{2+} concentrations to correlate the Ca-induced conformational changes and the complex stability.

We show here, for the first time, that the susceptibility of the loop between gelsolin segments 5 and 6 to limited proteolysis is diminished by Ca^{2+} in a concentration-dependent manner, with a full effect observed at >50 μM. This structural transition is accompanied by stabilization of actin binding. Thus, our data provide experimental proof for the suggestion (*14*) that binding of Ca^{2+} at low-affinity sites in gelsolin S4−6 produces conformational changes in the

† Supported by Deutsche Forschungsgemeinschaft SFB 549 and by the Program of the Russian Academy of Sciences on Physico-Chemical Biology.

* To whom correspondence should be addressed. Phone: 0049-521-1065616. Fax: 0049-521-1065654. E-mail: horst.hinssen@uni-bielefeld.de.

‡ Russian Academy of Sciences.

§ University of Bielefeld.

10.1021/bi049548z CCC: $27.50
Published on Web 09/14/2004

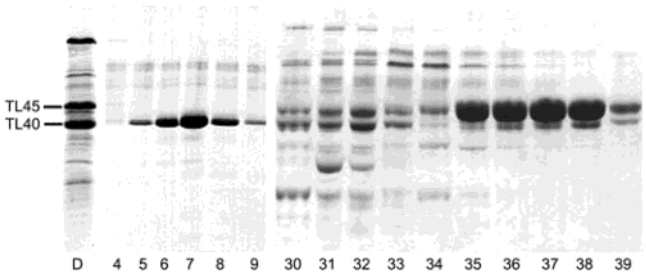

FIGURE 1: Separation of the C-terminal half of gelsolin (TL45) by anion-exchange chromatography on a Mono Q HR 5/5 column. TL45 was separated from the N-terminal half of gelsolin as described in Materials and Methods. TL40 appeared in the wash of the column (fractions 5−9); TL45 eluted at approximately 220 mM KCl (fractions 35−38).

loops around the Ca-binding sites, resulting in stabilization of actin−gelsolin interaction.

MATERIALS AND METHODS

Protein Preparations. Rabbit skeletal muscle actin was purified by the procedure of Spudich and Watt (*17*) with an additional gel filtration step on Sephadex G-150 to remove traces of actin-binding proteins. G-actin in buffer G (0.2 mM ATP, 0.1 mM $CaCl_2$, 0.4 mM β-mercaptoethanol, 5 mM Tris-HCl, pH 8.2, 1 mM NaN_3) was stored on ice and used within 1 week.

Gelsolin was isolated from pig stomach smooth muscle (*18*, *19*) and stored as an ammonium sulfate precipitate in liquid nitrogen. Before use, the precipitate was dissolved in PSAM buffer (10 mM imidazole, 0.5 mM EGTA,[1] 0.2 mM DTT, 2 mM NaN_3, pH 7.0) and dialyzed against the same buffer.

The C-terminal half of gelsolin (containing gelsolin segments 4−6, further called TL45) was obtained by limited proteolysis of gelsolin with thermolysin (*12*). Gelsolin (0.5−1.0 mg/mL) in PSAM buffer was activated by addition of 0.5 mM $CaCl_2$ to obtain 0.3 mM $CaCl_2$ in excess over EGTA, and the pH of the solution was adjusted to 7.2. Gelsolin was incubated with thermolysin at a weight ratio of 1:200 for 2−3 min at 25 °C. The reaction was terminated by addition of 10 mM EGTA. The precise time for optimal cleavage was determined for each batch of thermolysin.

The TL45 fragment was separated from the N-terminal half of gelsolin by anion-exchange chromatography on a Mono Q HR 5/5 column (Amersham). About 5 mg of the digest was applied to the column equilibrated with HPLC buffer containing 50 mM KCl, 1 mM $MgCl_2$, 1 mM EGTA, 0.2 mM DTT, and 20 mM imidazole, pH 7.0. TL45 was eluted from the column with a linear gradient of KCl (0.05−0.4 M) (Figure 1). The peak fractions were concentrated and dialyzed against PSAM buffer overnight.

Gel Chromatography. Analytical gel chromatography was performed using two columns of Superdex 200 HR 10/30 (Amersham) mounted in tandem on a Pharmacia FPLC system. To prepare the 1:1 actin/TL45 complexes, 0.5 mg of G-actin (in buffer G) was mixed with 0.5 mg of TL45 (in PSAM buffer), and the concentration of $[Ca^{2+}]$ in the mixture was adjusted to 0.2 mM. Aliquots of the mixture (100 μL) were applied to the columns equilibrated with 0.1 M KCl, 10 mM imidazole, pH 7.0, and $CaCl_2$/EGTA at various ratios and eluted with a corresponding buffer at a flow rate of 0.3 mL/min.

Limited Proteolysis. TL45 (0.5 mg/mL) either alone or as a complex with actin (0.5 mg/mL) was digested with trypsin at an enzyme:protein mass ratio of 1:5 at 22 °C. At different time points, the digestion was stopped by addition of soybean trypsin inhibitor, and the samples were analyzed by SDS−PAGE. Relative amounts of digested proteins were determined by densitometric quantification of Coomassie Blue stained gels using the program Phoretix (Molecular Dynamics).

SDS−Polyacrylamide Gel Electrophoresis. SDS−PAGE was performed using 15% acrylamide−0.1% bis(acrylamide) slab gels in the Laemmli buffer system (*20*).

Cross-Linking Experiments. For cross-linking of complexes between actin and the 29 kDa (segments 4−5) or 14 kDa (segment 6) fragments with EDC, TL45 was cleaved with trypsin at an enzyme:protein mass ratio of 1:20 for 60 min at 25 °C, and the reaction was terminated by addition of 2 mM TLCK. The digest (0.3 mg/mL) was mixed with a 3-fold amount of actin in the presence of 0.5 mM $CaCl_2$ and incubated with 4 mM EDC for 50 min at 25 °C (*21*). The reaction was stopped by the addition of the SDS−PAGE buffer, and cross-linking products were analyzed by SDS−PAGE.

Polypeptide Sequence Determination. TL45 fragments after limited proteolysis were separated by SDS−PAGE and transferred to PVDF membrane by semidry electroblotting. The blots were transiently stained with Ponceau S, and the bands of interest were cut out and subjected to automatic Edman degradation using a Knauer sequencer to obtain the N-terminal sequence of the respective polypeptides. To avoid misunderstandings, the numbering of the amino acids followed that of Burtnick et al. (*22*) for equine plasma gelsolin. Plasma gelsolin has an N-terminal extension of 25 amino acids; therefore, the first amino acid of the porcine cytoplasmic gelsolin used here is Val 26.

Molecular Modeling and Calculations. The program Swiss−Protein Database Viewer, version 3.6, was used for displaying and labeling the molecular structure of TL45. For modeling, the PDB files (1D0NB, 1H1V) for equine and human plasma gelsolins, respectively, were used from the data of refs *14* and *22* assuming bona fide that the structure of porcine cytoplasmic gelsolin used in our experiments is identical to that of equine and human gelsolin: In the relevant part of the molecule (segments 4−6) exchanges are present in only 12 positions. Since most of them are conservative exchanges, we have neglected these differences for modeling. $[Ca^{2+}]$ in Ca/EGTA mixtures was calculated using the program EQCAL (Biosoft).

RESULTS

Partial proteolytic cleavage of gelsolin by thermolysin initially yields two polypeptides with apparent molecular masses of 45 and 40 kDa (*23*), respectively. The 45 kDa fragment, called here TL45, represents the C-terminal half of gelsolin or segments 4−6. N-Terminal sequencing of

[1] Abbreviations: DTT, dithiothreitol; EDC, 1-ethyl-3-[3-(dimethylamino)propyl]carbodiimide; EGTA, ethylene glycol bis(β-aminoethyl)-*N*,*N*,*N*′,*N*′-tetraacetic acid; PAGE, polyacrylamide gel electrophoresis; SDS, sodium dodecyl sulfate; TLCK, N^{α}-tosyllysine chloromethyl ketone.

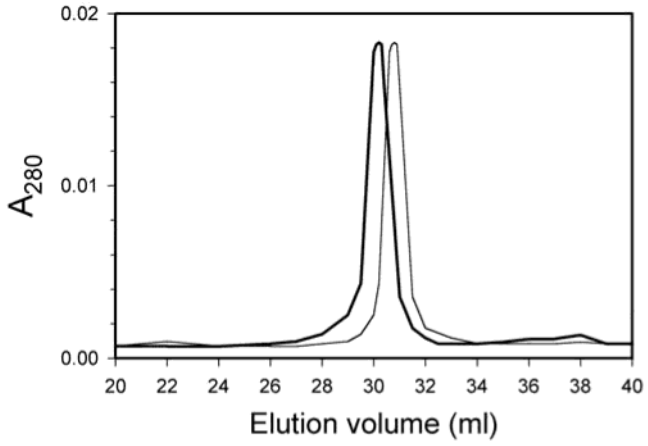

FIGURE 2: Effect of Ca^{2+} on the mobility of the C-terminal half of gelsolin during gel chromatography on Superdex 200 HR. 100 μL of TL45 (1 mg/mL) in 10 mM imidazole, 0.2 mM EGTA, 0.2 mM DTT, and 2 mM NaN_3, pH 7.0 (bold line), or in the same buffer complemented with 0.2 mM $CaCl_2$ in excess over EGTA (thin line) was applied to the columns equilibrated with 0.1 M KCl, 10 mM imidazole, pH 7.0, and 0.2 mM EGTA or 0.2 mM $CaCl_2$. The samples were eluted from the column with the corresponding buffer at a flow rate of 0.3 mL/min.

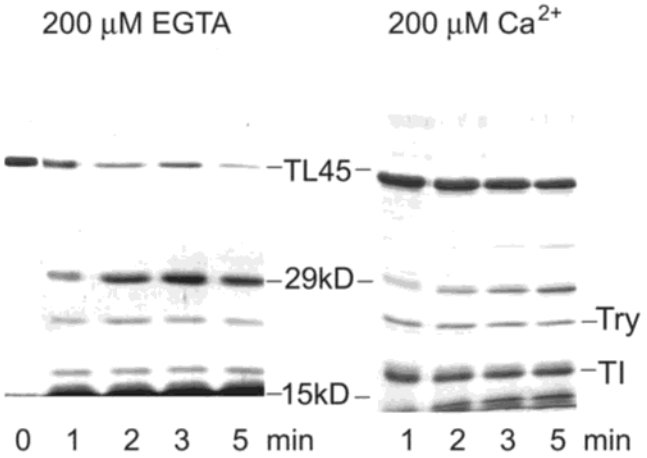

FIGURE 3: Cleavage of the C-terminal half of gelsolin with trypsin. 12 μM TL45 in 10 mM imidazole, 0.2 mM EGTA, 0.2 mM DTT, and 2 mM NaN_3, pH 7.0 (left part), or in the same buffer complemented with 0.2 mM $CaCl_2$ in excess over EGTA (right part) was cleaved with trypsin (Try) at an enzyme:protein mass ratio of 1:5. Proteolysis was stopped with soybean trypsin inhibitor (TI), and the samples were analyzed by SDS−PAGE at different time points after addition of trypsin.

isolated TL45 showed that the cleavage site for thermolysin is at Ile 387. The isolated fragment therefore contains 369 amino acids, and its actual molecular mass is 40.4 kDa. Assuming that segment 4 starts at Gln 419, according to the denomination of Burtnick et al. (*22*), the isolated fragment TL45 contains additional 30 amino acids of the loop connecting segments 3 and 4 (Figure 8).

Analytical Gel Filtration of TL 45 in the Presence and Absence of Ca^{2+}. Previously, the Ca-induced conformational changes in gelsolin and its C-terminal half were shown to be reflected in the decrease of the translational diffusion coefficient of the molecules, suggesting major rearrangements in the folding of the polypeptide chain (*12*, *24*). It may be expected that these structural transitions are also revealed by high-resolution gel chromatography. Indeed, under the conditions of gel filtration as used here, the elution volume of TL45 in EGTA was 30.2 mL, corresponding to a K_{av} of 0.598, whereas in the presence of 0.5 mM $CaCl_2$ it was increased to 30.8 mL (K_{av} of 0.622) (Figure 2). These data show that, under Ca conditions, the apparent size of TL45 is diminished most likely due to structural transitions, making the molecule more compact. Similarly, the modeling (Figure 9) shows that the EGTA conformation is more extended than the Ca conformation. To further confirm this effect of Ca^{2+} on the TL45 structure in solution, we have investigated its effect on limited proteolysis with trypsin.

Cleavage of TL 45 with Trypsin. Both in the absence and in the presence of $CaCl_2$, TL45 is cleaved with trypsin, yielding two fragments of ~29 and ~15 kDa, respectively (*5*, *10*) (Figure 3). After SDS−PAGE, the 15 kDa band was transferred to PVDF membrane, and its N-terminal amino acid sequence was determined as MDAHPP. In the known amino acid sequence of porcine gelsolin (*25*) this sequence corresponds to amino acids 635−640; therefore, the cleavage site is between Lys 634 and Met 635. In the 3D gelsolin structure (*22*), this site is located within the loop connecting segments 5 and 6. Thus, cleavage of TL45 by trypsin results in formation of segments 4−5 and segment 6.

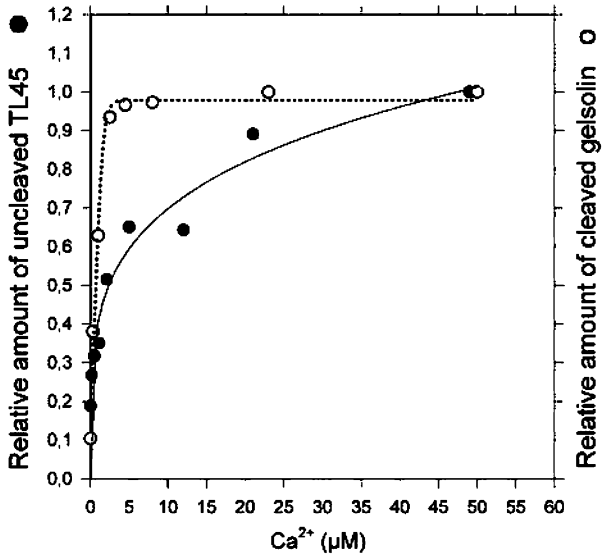

FIGURE 4: Comparison of the effects of Ca^{2+} on the susceptibility of gelsolin and its C-terminal half (segments 4−6) to tryptic proteolysis. TL45 (closed circles) and gelsolin (open circles) were cleaved with trypsin as described in the legend to Figure 3. Relative amounts of the digested gelsolin (open symbols) and undigested TL45 (closed symbols) were determined by densitometry of the Coomassie-stained gels.

Cleavage of TL45 with Trypsin at Different Ca Concentrations. As shown in both Figure 3 and the data presented in ref *10*, the cleavage site at Lys 634 is much more accessible to trypsin in the absence of Ca^{2+} than in its presence. Therefore, the disappearance of the TL45 band in the gel, accompanied by formation of the 29 kDa fragment, was used as a marker of Ca-induced structural transitions in TL45. Inhibition of the cleavage was observed already at 0.1 μM Ca^{2+}, was enhanced as [Ca^{2+}] was increased, and became maximal at about 100 μM Ca^{2+} (Figure 4). Comparison of these data with the susceptibility of the whole gelsolin molecule to trypsin (dotted line in Figure 4) indicates that the initial phase between 0.1 and 1 μM Ca^{2+} is part of

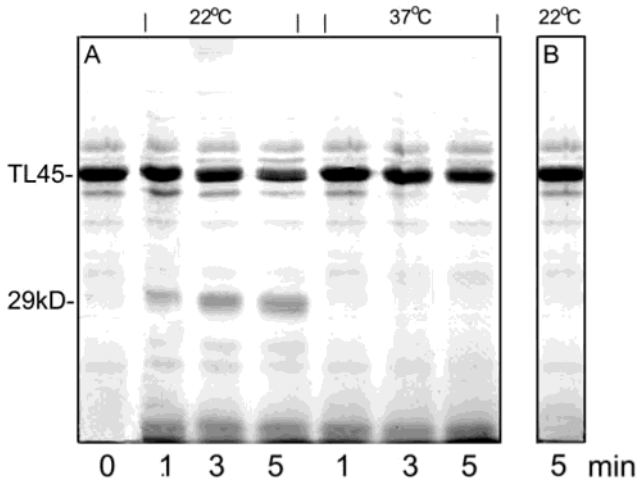

FIGURE 5: Effect of temperature on the susceptibility of the C-terminal half of gelsolin (TL45) to limited proteolysis with trypsin. (A) 12 μM TL45 at 12 μM [Ca^{2+}] was cleaved with trypsin at enzyme:protein mass ratios of 1:10 at 22 °C and 1:20 at 37 °C, respectively. Proteolysis was stopped with soybean trypsin inhibitor, and the samples were analyzed by SDS−PAGE at the time points indicated. (B) 12 μM TL45 was cleaved with trypsin at an enzyme: protein mass ratio of 1:10 and 22 °C in the presence of 200 μM [Ca^{2+}].

the general response of the gelsolin molecule, whereas high [Ca^{2+}] produces an additional effect, specific for TL45. Thus, the conformational changes that TL45 undergoes at 10^{-7} M Ca^{2+} are followed by additional structural transitions at 10^{-5}−10^{-4} M Ca^{2+}.

Effect of Temperature on the Cleavage of TL45 with Trypsin. As reported previously (*4*), Ca-induced activation of gelsolin is sensitive to increased temperature, and involvement of the tail helix latch in this regulation was suggested. This raises the question of whether sensitivity of gelsolin conformation to temperature is preserved in its C-terminal half. To address this issue, we compared the tryptic cleavage patterns of TL45 at 22 and 37 °C. To normalize the trypsin activity, trypsin concentration at 37 °C was two times lower than that at 22 °C (*26*). Figure 5 shows that, in contrast to a specific fragmentation of TL45 at 22 °C, at 37 °C the cleavage site at Lys 634 within loops 5−6 was strongly protected from proteolysis. This effect was observed in a whole range of Ca concentrations applied (not shown). Unspecific degradation of TL45 at the increased temperature did not allow quantitation of these data. Nevertheless, qualitatively the temperature-promoted protection of loops 5−6 closely resembles the effect produced by 100 μM Ca^{2+} at room temperature (Figure 5). This implies that both increased temperature and [Ca^{2+}] can produce similar rearrangements of gelsolin C-terminal segments.

Interaction of TL45 with Actin Probed by Limited Proteolysis. TL45 has one functional actin-binding site and can bind one actin monomer (*11*, *14*). To reveal the effect of [Ca^{2+}] on this binding, limited proteolysis with trypsin was used. In the presence of 200 μM Ca^{2+}, actin caused further inhibition of the cleavage within loops 5−6 (Figure 6). Concomitantly, cleavage of actin at Lys 68 was accelerated. This confirmed the formation of actin/TL45 complexes. The protective effect of actin did not depend on the type of divalent cation, Ca^{2+} or Mg^{2+}, bound at its high-affinity cation-binding site (Figure 6B). On the other hand, the effect of TL45 on Mg-actin appeared to be stronger than on Ca-actin (Figure 6B).

Figure 7 illustrates how cleavage of TL45 and actin within the complex depended on [Ca^{2+}]. The inhibitory effect of actin was more prominent at low Ca^{2+}, when TL45 is efficiently cleaved with trypsin. Surprisingly, some inhibition was observed even at [Ca^{2+}] as low as 0.01 μM (Figure 7A), raising a possibility that TL45 may weakly associate with actin even at very low Ca concentrations.

Stability of the TL45/Actin Complexes. When equimolar amounts of actin and TL45 were mixed at 200 μM Ca^{2+} and subjected to gel filtration, a single peak eluted at a position corresponding to a molecular mass of ∼80 kDa. SDS−PAGE of the peak fraction confirmed that, under these conditions, TL45 forms a stable 1:1 complex with actin (data not shown). Previously, we have used high-resolution gel chromatography to show that even though ternary actin/gelsolin complexes are formed at lower Ca^{2+}, they are unstable unless [Ca^{2+}] is >10 μM (*5*). To analyze whether at low Ca^{2+} the actin/TL45 complexes remain stable, similar gel filtration experiments were performed. Actin and TL45 were mixed in the presence of 200 μM Ca^{2+} at a 1:1 molar ratio. Aliquots of the mixture were applied on Superdex 200 columns which had been equilibrated with buffers containing different [Ca^{2+}] given in Table 1. The availability coefficient K_{av} of the complexes in the presence of 200 μM Ca^{2+} was 0.543, which was characteristic of a 1:1 actin/TL45 complex. In the presence of 200 μM EGTA (Ca^{2+} <0.01 μM), the availability coefficient was 0.589, equal to that of TL45 alone under these conditions. At intermediate [Ca^{2+}] the peaks were as distinct as for either the actin/TL45 complexes or TL45 alone. However, the peaks were recovered at intermediate elution volumes, giving the intermediate K_{av} values shown in Table 1. This difference can be accounted for by the fact that at Ca^{2+}<100 μM the preformed actin/TL45 complex was no longer stable and during chromatography gradually dissociated into TL45 and free actin. Since the dissociation seems to occur gradually during the run, the TL45 peaks eluted later than the intact actin/TL45 complexes but earlier than TL45 alone.

Hence the effect of Ca^{2+} on the stability of the actin/TL45 complexes is similar to that observed previously on the ternary actin/gelsolin complexes (*5*). However, stable complexes of TL45 with actin were formed only at [Ca^{2+}] of ∼100 μM, indicating that formation of stable actin/TL45 complexes requires higher [Ca^{2+}] than formation of ternary actin/gelsolin complexes.

Interaction of the 29 and 14 kDa Fragments with Actin. To reveal a role of different TL 45 segments in stabilization of TL45/actin complexes, we have investigated the interaction of the 29 and 14 kDa fragments from the tryptic digest of TL45 with actin. As judged from gel filtration experiments, no complexes with either of the fragments were formed at [Ca^{2+}] as high as 0.5 mM (data not shown). This indicates that integrity of TL45 is required for stable binding of the actin monomer to take place. These experiments do not exclude, however, the possibility of weak binding of actin to the 29/14 kDa peptides. To reveal possible weak interactions, cross-linking of the putative complexes with EDC was performed. Figure 8 shows several cross-linking products in the apparent molecular mass range of 48−65 kDa (Figure 8, lane 6) which are not present in the controls (Figure 8,

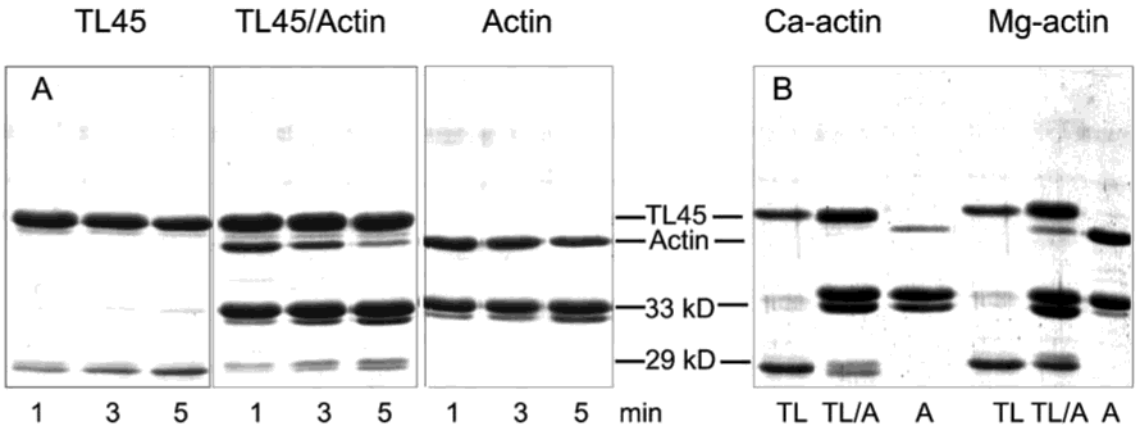

FIGURE 6: Effect of actin on the susceptibility of TL45 to proteolysis with trypsin. (A) 12 μM TL45 in 10 mM imidazole, 0.2 mM EGTA, 0.2 mM DTT, and 2 mM NaN_3, pH 7.0, was mixed with 12 μM skeletal muscle Ca−G-actin in buffer G, and the concentration of Ca^{2+} in the mixture was adjusted to 0.2 mM in excess over EGTA. The TL45/actin mixtures as well as 12 μM TL45 and 12 μM actin alone were digested with trypsin and analyzed as described in the legend to Figure 3. (B) Cleavage of 12 μM TL45 in the presence of 12 μM skeletal muscle Ca- or Mg-actin. Ca-actin was converted to Mg-actin by a 5 min incubation with 0.2 mM EGTA/0.1 mM $MgCl_2$.

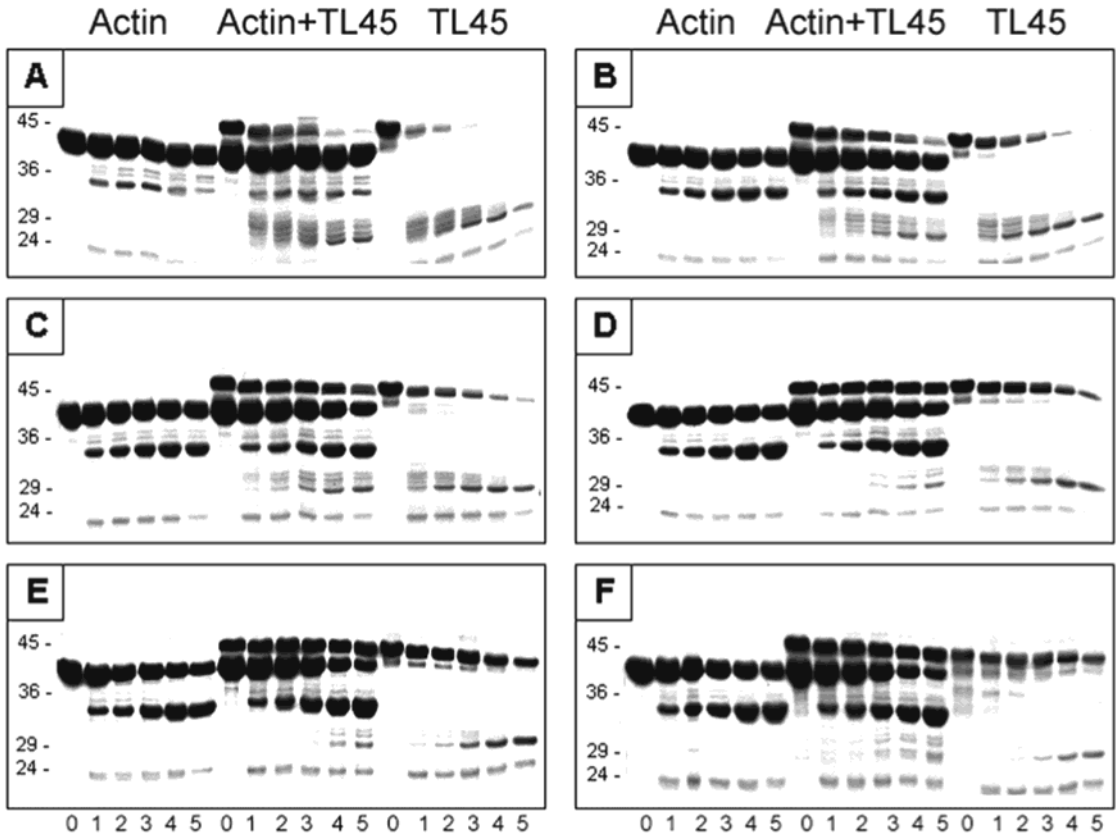

FIGURE 7: SDS−PAGE showing the additive effect of actin and of different concentrations of Ca^{2+} on the susceptibility of segments 4−6 of gelsolin to proteolysis with trypsin. TL45, actin, and TL45/actin complexes were cleaved with trypsin as described in the legends to Figures 3 and 5. Adjustment of Ca^{2+} in the solutions was made by adding different concentrations of $CaCl_2$ to 0.2 mM EGTA. The Ca concentrations in panels A, B, C, D, E, and F were <0.01, 10, 20, 50, 100, and 200 μM, respectively.

lanes 4 and 5), of which the lower ones might be complexes of the 14 kDa peptide with actin. It seems plausible, therefore, that in the presence of high [Ca^{2+}] actin forms an additional weak contact with the 14 kDa fragment (S6).

DISCUSSION

Activation of gelsolin at 0.1−1 μM Ca^{2+} involves opening of the molecule which allows one actin monomer to be bound (*2*−*5*). However, as we have previously shown, formation of a stable 2:1 actin/gelsolin complex occurs only at [Ca^{2+}] >10 μM (*5*). Interaction of actin monomer with the isolated N-terminal half of gelsolin is independent of Ca^{2+} (*11*). Moreover, there are apparently no major Ca-induced changes in the conformation of the N-terminal half of gelsolin, whereas a significant increase of the hydrodynamic volume of the C-terminal half was registered (*12*). We have therefore suggested previously (*5*) that binding of the second actin monomer in the ternary actin/gelsolin complex requires conformational transitions within segments 4−6 (the C-terminal half of gelsolin) taking place at high [Ca^{2+}]. To

Table 1: Gel Filtration of Preformed Actin/TL45 Complexes at Various [Ca^{2+}] on Superdex 200 HR[a]

[Ca^{2+}] (μM)	K_{av}	[Ca^{2+}] (μM)	K_{av}
<0.01	0.598	50	0.559
10	0.583	100	0.543
20	0.567	200	0.543

[a] A mixture (100 μL) of actin and gelsolin at a stoichiometric ratio of 2:1 in 200 μM Ca^{2+} was applied to a set of 2 × 30 cm columns mounted in tandem. The columns were equilibrated with buffer containing the Ca^{2+} concentrations given in the table and eluted at 0.3 mL/min. K_{av} values were calculated using the formula $K_{av} = (V'_e - V_0)(V_t - V_0)^{-1}$, where V_e is the elution volume of the component, V_0 the void volume, and V_t the total volume of the column.

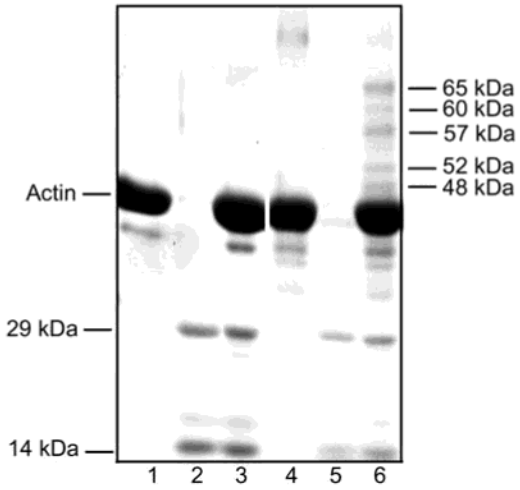

FIGURE 8: Cross-linking of actin with the 29 and 14 kDa fragments. Actin (1 mg/mL) in buffer G was mixed with a 0.3 mg/mL 29/14 kDa mixture in 10 mM imidazole, 0.2 mM EGTA, 0.2 mM DTT, and 2 mM NaN_3, pH 7.0, and the concentration of Ca^{2+} in the mixture was adjusted to 0.2 mM in excess over EGTA. Cross-linking with EDC was performed as described in Materials and Methods. Lanes 1−3: controls, actin (1), TL45 digest (2), and mixture of both (3). Lanes 3−6: the corresponding proteins after 50 min cross-linking.

prove this hypothesis, we have isolated the C-terminal half of gelsolin after proteolysis with thermolysin and analyzed its conformation and interaction with monomeric actin in response to Ca^{2+} using the same approach as previously for analysis of the whole gelsolin (*5*). Our data showed that the complex between the C-terminal half of gelsolin and actin is stable only at Ca^{2+} >100 μM, which correlates with the conformational changes observed in this [Ca^{2+}] range.

The site cleaved with trypsin in TL45 is located in the loop connecting segments 5 and 6 (Figure 9). In general, exposure of the loop in the Ca-free (*13*) and Ca-activated (*14*−*16*) gelsolin segments 4−6 is rather similar. Our data show, however, that binding of Ca^{2+} results in burying the site at Lys 634, indicating a Ca-induced folding of loops 5−6. These data are consistent with and confirm movement of segment 5 to a new position, in which it establishes a tighter association with segment 6, the shift that may result from the replacement by calcium of a salt bridge between Asp 565 and Arg 629 (*15*). Similar burying of the site at Lys 634 can be produced by elevated temperature. Previously, the temperature-dependent activation of gelsolin was discussed only in terms of the tail−helix−latch hypothesis (*4*, *27*). Our results show that specific regulation of gelsolin by temperature is preserved in its C-terminal half, suggesting that the temperature-induced unlatching may be accompanied by further interdomain rearrangements.

Calcium-driven rearrangements of segments 4−6 can also affect actin binding. It is known that S4−6 binds one actin monomer, and the binding site is located in S4 (for a recent review, see ref *1*). However, S4−5 binds G-actin 50 times weaker than S4−6 and only at strongly increased [Ca^{2+}] (*28*). Moreover, in the polymerization inhibition assay no inhibitory effect by S4 was observed, indicating that the presence of S6 is indispensable for high-affinity interaction (*28*). Analysis of the S4−6/actin crystal structure (*14*) also suggested the appearance of the new interface between the Ca-modified surface of segment 6 and actin. Such an additional actin/S6 contact could account for the observed cross-linking between actin and S6 and the higher stability of actin/TL45 complexes in high [Ca^{2+}] as demonstrated in our work.

Binding of actin appears to produce additional transitions of the gelsolin structure. Interaction of actin monomer with segment 6 unlikely causes steric inhibition of cleavage at Lys 634 since the cleavage site and actin are located on the opposite sides of segments 4−6 (Figure 8). Comparison of the segment 4−6 crystal structure derived from the structure of the S4−6/actin complex (*14*) with those for actin-free S4−6 (*15*, *16*) reveals only a minor shift in the position of loops 5−6 in the complex. We therefore suppose that a significant effect on the accessibility of loops 5−6 shown in our work is caused by actin-induced conformational transitions that are stronger in solution than in the crystal structure. Similar effects can be relevant for the whole gelsolin molecule. In the whole gelsolin, either Ca-free or Ca-activated, the site between Lys 634 and Met 635 seems to be inaccessible for trypsin (*5*). However, cleavage of gelsolin at the same site with formation of segments 1−5 and segment 6 occurred upon actin binding (5). Moreover, stable binding of a second actin monomer in ternary actin/gelsolin complexes was observed at lower [Ca^{2+}] than formation of stable actin/TL45 complexes. It is therefore tempting to speculate that binding of the actin monomer in the N-terminal half of gelsolin promotes Ca-dependent changes in segments 5 and 6 which stabilize binding of the second actin monomer which is known to be a cooperative process (*29*).

In turn, binding of TL45 apparently makes Lys 68 in the nucleotide-containing cleft of actin more accessible to trypsin cleavage. This indicates that, in the actin monomer bound to TL45, either the nucleotide-binding cleft is more open to solvent (for a review, see ref *30*) or a structural transition of segments 61−68 takes place. Interestingly, the crystal structure of actin in the complex with gelsolin segments 4−6 (*14*) differs from the known actin structures (*31*−*34*), since it shows an unstructured region in amino acids 61−68 versus a β-sheet in the other models. Although different resolution of the different models does not permit a direct correlation of our biochemical data with the structural information, these data correlate with a low nucleating activity of the C-terminal half of gelsolin (data not shown). We have shown earlier that binding of the whole gelsolin molecule and of its N-terminal half induced allosteric effects within the DNase I binding loop of actin and that this effect may be significant for gelsolin-induced nucleation of actin polymerization (*35*). The effect of TL45 on actin structure emphasizes again that

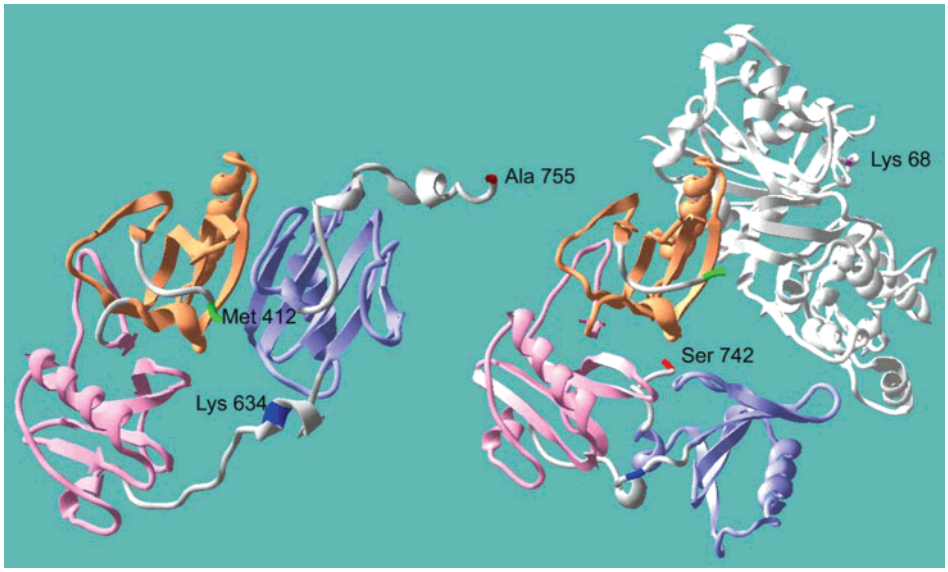

FIGURE 9: Structural model of the C-terminal half (starting from Met 412) of gelsolin containing segments 4 (orange), 5 (pink), and 6 (blue) either in the Ca^{2+}-free state (left) or in the presence of Ca^{2+} with one actin molecule bound to it (right). The data of Robinson et al. (*13*) were used for the Ca^{2+}-free model, and the data of Choe et al. (*14*) were used for the gelsolin−actin complex. For orientation, the N-terminal amino acids are colored green, and the C-terminal amino acids are in red. The position of Lys 634, the cleavage site for trypsin, is colored blue, and on the actin molecule, Lys 68 is colored purple. Please note that the Ca-free model ends at Ala 755, whereas in the complex the gelsolin data end at Ser 742.

gelsolin-induced conformational changes in actin may contribute to the gelsolin activities toward actin.

Structural analysis predicted the existence of a Ca-binding site in every segment of the S4−6/actin complex (*14*), and it was shown that the Ca-activated actin-free C-terminal half of gelsolin crystallized in the presence of 1 mM $CaCl_2$ contains three calcium ions (*16*). On the other hand, measurements of calcium binding to gelsolin segments 4−6 revealed a maximum stoichiometry of 2 Ca^{2+}/mol of protein (*2*). In line with this, two calcium ions were found in domains 5 and 6, one in each, in the Ca-activated actin-free structure of segments 4−6 crystallized in the presence of 0.1 mM $CaCl_2$, whereas binding of calcium in subdomain 4 was suggested to depend on subsequent actin binding (*15*). This discrepancy may be due to a difference in the calcium concentrations used in these experiments. Our data show that Ca-associated protection of the cleavage site at Lys 634 at >50 μM [Ca^{2+}] is similar to the effect induced by binding of actin at micromolar [Ca^{2+}]. This raises the possibility that at micromolar [Ca^{2+}] actin can induce structural transitions in segments 4−6 followed by binding additional calcium ions (*36*) and adopting a functionally relevant conformation.

According to equilibrium dialysis experiments, segments 4−5 bound Ca^{2+} with a K_d of 2 μM, thereby the saturation occurred at about 20 μM Ca^{2+} (*2*). Also, oxidation of gelsolin amino acid residues by synchrotron radiation was accelerated significantly at 1−5 μM Ca^{2+} followed by a further acceleration step with a midpoint of 60−100 μM [Ca^{2+}]. These data are consistent with a three-stage activation process (*36*). In a good agreement with these values, our data indicate that >100 μM [Ca^{2+}] is required to promote final conformational changes in loops 5−6 and to stabilize actin binding. Taken together, these data suggest that binding of the second actin monomer in the actin/gelsolin ternary complex is stabilized by binding of calcium to the low-affinity site(s) involving gelsolin segment 5.

REFERENCES

1. McGough, A. M., Staiger, C. J., Min, J. K., and Simonetti, K. D. (2003) The gelsolin family of actin regulatory proteins: modular structures, versatile functions, *FEBS Lett. 552*, 75−81.
2. Pope, B., Gooch, J., and Weeds, A. G. (1997) Probing the effects of calcium on gelsolin, *Biochemistry 36*, 15848−15855.
3. Kinosian, H. J., Newman, J., Lincoln, B., Selden, L. A., Gershman, L. C., and Estes, J. E. (1998) Ca^{2+} regulation of gelsolin activity: binding and severing of F-actin, *Biophys. J. 75*, 3101−3109.
4. Lin, K. M., Mejillano, M., and Yin, H. L. (2000) Ca^{2+} regulation of gelsolin by its C-terminal tail, *J. Biol. Chem. 255*, 27746−27752.
5. Khaitlina, S., and Hinssen, H. (2002) Ca-dependent binding of actin to gelsolin, *FEBS Lett. 521*, 14−18.
6. Lamb, J. A., Allen, P. G., Tuan, B. Y., and Janmey, P. A. (1993) Modulation of gelsolin function. Activation at low pH overrides Ca^{2+} requirement, *J. Biol. Chem. 268*, 8999−9004.
7. Allen, P. G., and Janmey, P. A. (1994) Gelsolin displaces phalloidin from actin filaments. A new fluorescence method shows that both Ca^{2+} and Mg^{2+} affect the rate at which gelsolin severs F-actin, *J. Biol Chem. 269*, 32916−32923.
8. Ditsch, A., and Wegner, A. (1995) Two low-affinity Ca(2+)-binding sites of gelsolin that regulate association with actin, *Eur. J. Biochem. 229*, 512−516.
9. Irobi, E., Burtnick, L. D., Urosev, D., Narayan, K., and Robinson, R. C. (2003) From the first to the second domain of gelsolin: a common path on the surface of actin?, *FEBS Lett. 552*, 86−90.
10. Lagarrigue, E., Maciver, S. K., Fattoum, A., Beniamin, Y., and Roustan, C. (2003) Co-operation of domain-binding and calcium-binding sites in the activation of gelsolin, *Eur. J. Biochem. 270*, 2236−2243.
11. Bryan, J. (1988) Gelsolin has three actin-binding sites, *J. Cell Biol. 106*, 1553−1562.
12. Hellweg, T., Hinssen, H., and Eimer, W. (1993) The Ca(2+)-induced conformational change of gelsolin is located in the carboxyl-terminal half of the molecule, *Biophys. J. 65*, 799−805.
13. Robinson, R. C., Mejillano, M., Le, V. P., Burtnick, L. D., Yin, H. L., and Choe, S. (1999) Domain movement in gelsolin: a calcium-activated switch, *Science 286*, 1939−1942.
14. Choe, H., Burtnick, L. D., Mejillano, M., Yin, H. L., Robinson, R. C., and Choe, S. (2002) The calcium activation of gelsolin: insights from the 3A structure of the G4-G6/actin complex, *J. Mol. Biol. 324*, 691−702.

15. Kolappan, S., Gooch, J. T., Weeds, A. G., and McLaughlin, P. J. (2003) Gelsolin domains 4−6 in active, actin-free conformation identifies sites of regulatory calcium ions, *J. Mol. Biol. 329*, 85−92.
16. Narayan, K., Chumnarnsilpa, S., Choe, H., Irobi, E., Urosev, D., Lindberg, U., Schutt, C. E., Burtnick, L. D., and Robinson, R. C. (2003) Activation in isolation: exposure of the actin-binding site in the C-terminal half of gelsolin does not require actin, *FEBS Lett. 552*, 82−85.
17. Spudich, J. A., and Watt, S. (1971) The regulation of rabbit skeletal muscle contraction 1. Biochemical studies of the interactions of the tropomyosin-troponin complex with actin and the proteolytic fragments of myosin, *J. Biol. Chem. 246*, 4866−4871.
18. Hinssen, H., Small, J. V., and Sobieszek, A. (1984) A Ca^{2+}-dependent actin modulator from vertebrate smooth muscle, *FEBS Lett. 165*, 90−95.
19. Pope, B., Gooch, J., Hinssen, H., and Weeds, A. G. (1989) Loss of calcium sensitivity of plasma gelsolin is associated with the presence of calcium ions during preparation, *FEBS Lett. 259*, 185−188.
20. Laemmli, U. K. (1970) Cleavage of structural proteins during the assembly of the head of bacteriophage T4, *Nature 227*, 680−685.
21. Sutoh, K., and Yin, H. L. (1989) End-label fingerprinting show that the N- and C-termini of actin are in the contact site with gelsolin, *Biochemistry 28*, 5269−5275.
22. Burtnick, L. D., Koepf, E. K., Grimes, J., Jones, E. Y., Stuart, D. I., McLaughlin, P., and Robinson, C. R. (1997) The crystal structure of plasma gelsolin: implications for severing, capping and nucleation, *Cell 90*, 661−670.
23. Chaponnier, C., Janmey, P. A., and Yin, H. L. (1986) The actin filament-severing domain of plasma gelsolin, *J. Cell Biol. 103*, 1473−1481.
24. Patkowski, A., Hinssen, H., and Dorfmüller, T. (1990) Size, shape parameters, and Ca^{2+}-induced conformational change of the gelsolin molecule: A dynamic light scattering study, *Biopolymers 30*, 427−435.
25. Way, M., and Weeds, A. (1988) Nucleotide sequence of pig plasma gelsolin. Comparison of protein sequence with human gelsolin and other actin-severing proteins shows strong homologies and evidence for large internal repeats, *J. Mol. Biol. 203*, 1127−1133.
26. Stevens, E. D., and McLeese, J. M. (1984) Why bluefin tuna have warm tummies: temperature effect on trypsin and chymotrypsin, *Am. J. Physiol. 246*, R487−R494.
27. Cheng, F., Shen, J., Luo, X., Jiang, H., and Chen, K. (2002) Steered molecular dynamics simulation on the "tail helix latch" hypothesis in the gelsolin activation process, *Biophys. J. 83*, 753−762.
28. Pope, B., Maciver, S., and Weeds, A. (1995) Localization of the calcium-sensitive actin monomer binding site in gelsolin to segment 4 and identification of calcium binding sites, *Biochemistry 34*, 1583−1588.
29. Hinssen, H. (1987) Actin-modulating proteins. Complex formation and Ca^{2+}-dependence of interaction with actin, *Prog. Zool. 34*, 53−63.
30. Strzelecka-Golaszewska, H. (2001) Divalent cations, nucleotides, and actin structure, *Results Probl. Cell Differ. 32*, 23−4127.
31. Kabsch, W., Mannherz, H. G., Suck, D., Pai, E. F., and Holmes, K. C. (1990) Atomic structure of the actin: DNase I complex, *Nature 347*, 37−44.
32. McLaughlin, P. J., Gooch, J. T., Mannherz, H. G., and Weeds, A. G. (1993) Structure of gelsolin segment 1-actin complex and the mechanism of filament severing, *Nature 364*, 685−692.
33. Otterbein, L. R. C., Graceffa, P., and Dominguez, R. (2001) The crystal structure of uncomplexed actin in the ADP state, *Science 293*, 708−711.
34. Klenchin, V. A., Allingham, J. S., King, R., Tanaka, J., Marriott, G., and Rayment, I. (2003) Trisoxazole macrolide toxins mimic the binding of actin-capping proteins to actin, *Nat. Struct. Biol. 10*, 1058−1063.
35. Khaitlina, S., and Hinssen, H. (1997) Conformal changes in actin induced by its interaction with gelsolin, *Biophys. J. 73*, 929−937.
36. Kiselar, J. G., Janmey, P. A., Almo, S. C., and Chance, M. R. (2003) Visualizing the Ca^{2+}-dependent activation of gelsolin by using synchrotron footprinting, *Proc. Natl. Acad. Sci. U.S.A. 100*, 3942−3947.

BI049548Z